pubs.acs.org/Biomac

Article

Lipase-Catalyzed Synthesis and Characterization of Poly(glycerol sebacate)

Zhuoyuan Ning,[#] Kening Lang,[#] Ke Xia, Robert J. Linhardt, and Richard A. Gross*

Cite This: *Biomacromolecules* 2022, 23, 398–408

Read Online

ACCESS | Metrics & More | Article Recommendations | Supporting Information

ABSTRACT: This study demonstrated that immobilized *Candida antarctica* lipase B (N435) catalysis in bulk leads to higher molecular weight poly(glycerol sebacate), PGS, than self-catalyzed condensation polymerization. Since the glass-transition temperature, fragility, modulus, and strength for rubbery networks are inversely dependent on the concentration of chain ends, higher molecular weight PGS prepolymers will enable the preparation of cross-linked PGS matrices with unique mechanical properties. The evolution of molecular species during the prepolymerization step conducted at 120 °C for 24 h, prior to enzyme addition, revealed regular decreases in sebacic acid and glycerol-sebacate dimer with corresponding increases in oligomers with chain lengths from 3 to 7 units such that a homogeneous liquid substrate has resulted. At 67 h, for N435-catalyzed PGS synthesis, the carboxylic acid conversion reached 82% without formation of a gel fraction, and number-average molecular weight (M_n) and weight-average molecular weight (M_w) values reached 6000 and 59 400 g/mol, respectively. In contrast, self-catalyzed PGS condensation polymerizations required termination at 55 h to avoid gelation, reached 72% conversion, and M_n and M_w values of 2600 and 13 800 g/mol, respectively. We also report the extent that solvent fractionation can enrich PGS in higher molecular weight chains. The use of methanol as a nonsolvent increased M_n and M_w by 131.7 and 18.3%, respectively, and narrower dispersity ($Đ$) decreased by 47.7% relative to the nonfractionated product.

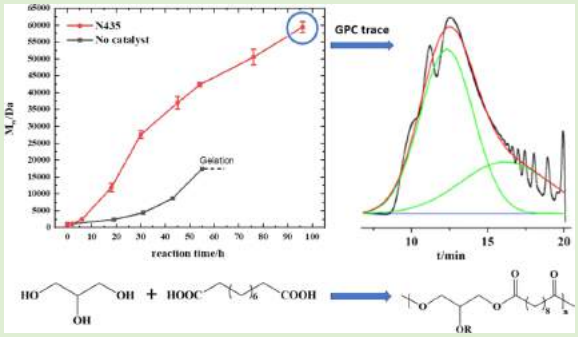

INTRODUCTION

Given the human body's complexity and the wide range of requirements in regenerative medicine, a biomaterial design would benefit by building in structural and functional diversity. Furthermore, biodegradable polymeric materials are preferred for three-dimensional tissue engineering scaffolds, drug delivery, bioadhesives, and various temporal implants. Another important attribute of the biomaterial design is the ability to functionalize biomaterials with various biological factors to control biological processes such as accelerating wound healing and regulating inflammatory processes.[1−3]

Herein, we focus on aliphatic biodegradable polyol polyesters, a family of synthetic biomaterials that generally consist of a polyol and diacids such as glycerol,[4−25] sorbitol,[18,23−27] xylitol,[18,28] mannitol,[18,28] sebacic acid,[4−18] adipic acid,[22−24,27,29,30] and suberic acid.[31] They were designed to provide a wide range of therapeutic functions. Examples include polyesters to support osteogenic differentiation and bone tissue regeneration,[16,32] osteoinductive scaffolds as growth media for preosteoblasts,[4] scaffolds that are conducive to the growth of 3T3 fibroblasts,[5,15] drug delivery systems with antiliver cancer activity,[33] fibers to instruct donor and host cells in cardiac patch applications,[6] pressure sensor arrays for cardiovascular monitoring, pressure-assisted wound healing and traumatic brain injury,[7] delivery of functional cardiomyocytes for myocardial infarction recovery,[34] nanofibers to promote nerve stem cell proliferation,[10] vocal fold scaffolds for cell proliferation,[11] scaffold for the growth of muscle cells,[12] and subcutaneous fat tissue.[13]

Poly(glycerol sebacate), PGS,[35,36] was first reported by Wang and co-workers in 2002.[15] The hydrolytic degradation products of PGS result in the natural metabolite's glycerol and sebacic acid. Sebacic acid is normally found in urine, and glycerol is a natural metabolite formed by hydrolysis of plant- and animal-derived triglycerides.[37,38] In addition, PGS is approved for biomedical use by the Food and Drug Administration, reducing the timeline for the approval of PGS-based biomaterials for clinical studies.[6]

Cross-linked PGS has been described as having elastomeric mechanical properties, causing negligible inflammation consistent with good biocompatibility.[4,14,15,17,39] Unlike conventional polyesters such as poly(lactic acid) that degrade by bulk

Received: October 13, 2021
Revised: December 5, 2021
Published: December 22, 2021

erosion, where strength loss precedes weight loss, PGS hydrolyzes via a surface erosion mechanism with concurrent losses in both weight and strength.[39] These features of PGS, which lead toward a linear hydrolytic weight loss rate, have been exploited for the controlled release of drug-laden PGS.[5,6,15,18,32,34,39−41] Furthermore, the elastomeric material properties of PGS have led to its use as matrices for soft material tissue engineering of retinal, adipose, cardiac, nerve, and vascular applications.[5,17]

Generally, the two routes for PGS synthesis are by ring opening of diglycidyl sebacate epoxy moieties by a reaction with the carboxylic acid functionalities of sebacic acid and by the direct copolymerization of glycerol and sebacic acid.[42,43] The former method normally leads to PGS with lower $Đ$, less branching, and avoids high vacuum in the polymerization step. However, the synthesis of diglycidyl sebacate involves the condensation of acyl chloride and glycidol, which is relatively expensive, results in a moderate monomer yield (∼70%), and requires monomer purification steps. The other established synthetic method is by the bulk condensation polymerization of glycerol and sebacic acid without catalyst addition (i.e., self-catalyzed).[12,44] Literature protocols generally involve a first oligomerization step known as the prepolymerization period or step where glycerol and sebacic acid undergo condensation reactions in bulk under a nitrogen atmosphere for 24 h at 120−140 °C.[5,6,10−15,17,18,45−54] Subsequently, to increase the rate of propagation, the reaction temperature is maintained at 120−150 °C under reduced pressure (e.g., 40 mTorr) for 4 h to 7 days. The problem encountered with the later synthetic approach is that, as the functional group conversion increases, a gel is formed.[46,55] Careful monitoring of product viscosity is required to inform when the reaction must be quenched to avoid gelation.[18] The resulting syrupy prepolymer has reported molecular weight values that range from 500 to 6300 g/mol for M_n and 1100 to 17 700 g/mol for M_w.[5,10,13,17,45,47,49,52−54,56] These prepolymers are then cross-linked in the absence of additives by heating at 120−150 °C for 4−168 h under vacuum.[5,6,10−15,17,18,45−54] To enhance the properties of cross-linked PGS biomaterials, other components have been incorporated into the cross-linked matrices. Representative examples include nanosilicates,[4] poly(butylene succinate-dilinoleate),[57] β-tricalcium phosphate,[58] and graphene for piezoresistive sensors.[48]

The use of a regioselective lipase catalyst could avoid cross-linking reactions, enabling the synthesis of higher molecular weight PGS. Due to its promiscuity, high thermal stability, activity, and seemingly contradictory regio-, chemo-, and enantioselectivity, *Candida antarctica* lipase B (CALB) has been the enzyme of choice for polycondensation polymerizations.[32,42,59,60] Novozyme 435 (N435) is the primary immobilized CALB catalyst used. It is composed of CALB that has been physically immobilized in a poly(methyl methacrylate-co-butyl methacrylate) (PMMA) resin.[59]

Our group, as well as others, reported N435-catalyzed copolymer syntheses in bulk using aliphatic diols, polyols, and diacids as monomers.[3,19−30,61−63] Investigations have included variables such as a monomer structure, reaction temperature, medium (solvent vs bulk), and catalyst concentration on the polymerization rate, chain structure, and molecular weight averages.[19,22−25,30] For example, copolymers of glycerol, 1,8-octanediol, and adipic acid (1:0.8:0.2 equiv) were prepared by N435 catalysis in bulk at 70 °C for 42 h, resulting in hyperbranched copolymers with M_w 75 600 g/mol and $Đ$ 2.9.[22] Another example is the N435-catalyzed synthesis of unsaturated polyesters by copolymerization of 1,18-*cis*-9-octanedecenedioic acid, glycerol, and linoleic acid. When the molar ratio was 1:1:0.67, in 9 h, the M_n and $Đ$ reached 9500 g/mol and 4.5, respectively.[19]

Previous research on PGS synthesis focused on the preparation of PGS prepolymers without catalyst addition. While molecular weights have been reported, most literature sources do not reveal size-exclusion chromatography (SEC) traces as well as a characterization of chain dispersity. Furthermore, with few exceptions, chain growth as a function of reaction times has not been reported. Also, there are lack of efforts to define the products of the prepolymerization step and to better define the product molecular weight by peak deconvolution of SEC traces.[5,18]

This study explored the hypothesis that N435 selectivity is sufficient, under the reaction conditions used, to avoid cross-linking reactions, enabling the synthesis of higher molecular weight PGS. Higher molecular weight PGS would provide a route to unique PGS materials that, after cure, could provide improved mechanical properties. It has been reported that properties such as the glass-transition temperature, fragility, modulus, and strength for rubbery networks that result from the curing step are inversely dependent on the concentration of chain ends.[64] Also, strands in the network terminating in a free chain end are ineffective elastically such that mechanical energy dissipation (hysteresis) is dependent on the chain length. It follows that, as the chain length exceeds a critical value, the concentration of chain ends becomes so low that further increases in chain length have negligible effects on matrix properties. This underlines the importance of developing routes to higher molecular weight PGS.

This paper reports comparisons between the molecular weight, functional group conversion, and substitution of glycerol repeat units as a function of time for self-catalyzed and N435-catalyzed PGS synthesis by SEC and nuclear magnetic resonance (NMR) analyses. Deconvolution of product SEC traces was used to better define the proportion of products that reside in different regions of SEC traces. Furthermore, to better understand the composition of products formed during the prepolymerization period at 120 °C for 24 h, analysis by electrospray ionization-mass spectrometer (ESI-MS) was performed. In addition, a PGS microstructure was defined by ^{1}H and ^{13}C NMR studies. Also, to further increase the PGS molecular weight, fractionation by solvent precipitation was carried out.

EXPERIMENTAL METHODS

Materials. Glycerol, sebacic acid, and solvents were purchased from Sigma-Aldrich in the highest available purity. Deuterated NMR solvents were purchased from Acros Organics. Immobilized CALB (N435) was a gift from Novozymes (Bagsværd, Denmark).

Self-Catalyzed Synthesis of PGS. Equimolar quantities of glycerol (15.64 g, 0.17 mol) and sebacic acid (34.36 g, 0.17 mol) were transferred to a 500 mL round-bottom flask. First, the reaction mixtures were maintained at 150 °C under a nitrogen atmosphere for 1 h. The resulting monophasic liquid was maintained at 120 °C for 24 h (prepolymerization conditions) and, thereafter, the reaction temperature and pressure were maintained at 120 °C and 2.5 Torr, respectively, for another 67 h.

N435-Catalyzed Synthesis of PGS. N435-catalyzed polymerizations of equimolar glycerol and sebacic acid were conducted in a 500 mL round-bottom flask. The reaction mixture was maintained at 150 °C under a nitrogen atmosphere using magnetic stirring for 1 h.

https://doi.org/10.1021/acs.biomac.1c01351
Biomacromolecules 2022, 23, 398−408

The resulting monophasic bulk reaction mixture was incubated at 120 °C for 24 h (prepolymerization). These steps mimicked those above and were conducted without the addition of N435. Then, the reaction temperature was brought to 90 °C, N435 (10 wt % relatives to the total weight of monomers) was added, and these conditions were maintained for 2 h under a nitrogen atmosphere. The flask was then connected to a vacuum pump, and the pressure was maintained at 100 Torr. After 4 h, the pressure was decreased to 75 Torr for 12 h, 50 Torr for 12 h, and finally, 25 Torr for 67 h before the reaction was stopped. Crude products were dissolved in chloroform, and the N435 beads were removed by filtration under reduced pressure. The chloroform was evaporated to give light-yellow viscous liquids.

Gel Permeation Chromatography. Analysis was performed using tetrahydrofuran (THF) as the eluent, at 40 °C, via a Waters SEC system equipped with a Waters 1515 HPLC pump, a Waters 2707 autosampler, a Waters 2414 differential refractive index detector, and a cascade of two Waters ResiPore columns (300 × 7.5 mm^2, model numbers PL1113-6300 and PL1110-6530) at a flow rate of 1.0 mL/min. The number- and weight-average molecular weight values (M_n and M_w, respectively), as well as the molecular mass dispersity ($Đ_M = M_w/M_n$), were determined relative to polystyrene standards.

Nuclear Magnetic Resonance (NMR) Spectroscopy. ^{1}H NMR spectra were recorded using a 500 MHz Agilent spectrometer, and ^{13}C NMR spectra were recorded with a Bruker 600 MHz spectrometer. NMR analyses were performed at 25 °C with $(CD_3)_2CO$ and $CDCl_3$ as the solvent. The tetramethylsilane (TMS) peaks at 0.00 ppm were used as an internal standard.

Electrospray Ionization-Mass Spectrometry (ESI-MS). High-resolution ESI-MS analyses were conducted on a Thermo LTQ XL Orbitrap (Bremen, Germany). Mobile phase A consisted of 5 mM ammonium acetate aqueous solution prepared with HPLC grade water. Mobile phase B consisted of 5 mM ammonium acetate prepared with HPLC grade acetonitrile and water (98 and 2 vol %, respectively). After injection of 5.0 μL samples by an Agilent 1200 autosampler, a single mobile phase of 50% HPLC grade acetonitrile in 5 mM ammonium acetate was used at a flow rate of 250 μL/min. The optimized parameters used included a spray voltage of 4.2 kV, a capillary voltage of −40 V, a tube lens voltage of −50 V, a capillary temperature of 275 °C, a sheath flow rate of 40 au, and an auxiliary gas flow rate of 20 au. All mass spectra were acquired at a resolution of 60 000 g/mol with a 180−1800 g/mol mass range.

Fractional Precipitation of Crude PGS. Crude PGS products (500 mg) were dissolved in THF (1 mL), and the solution was mixed on a vortex spinner for 5 min. Precipitation of crude PGS-THF solutions was conducted by slow addition to those solutions of cold preselected alcohol (9 mL). Then, turbid THF−alcohol mixtures were refrigerated at −20 °C for 16 h. Subsequently, the supernatant was removed by centrifugation, and the solvent contained in the precipitant was removed at 50 °C in a vacuum oven for 24 h. The weight fraction and average molecular weight values of fractionated products are also investigated.

RESULTS AND DISCUSSION

ESI-MS Analysis of PGS Prepolymers. ESI-MS provided insights into the growth of oligomeric species during the time when the reactants were maintained at 150 °C under a nitrogen atmosphere for 1 h and, thereafter, 120 °C for 24 h. The rationale for these steps is to convert the solid sebacic acid (melting point 131−134.5 °C)[65] to low molecular weight oligomers that is a liquid at 90 °C. Hence, this homogenous liquid is compatible with the retaining N435 activity during condensation polymerizations.[66] In other words, the heterogeneity of reactions consisting of an insoluble catalyst and substrate would lead to unfavorable reaction kinetics.

While such prepolymerization periods prior to N435 catalysis are common practices, information on changes in molecular species as a function of incubation time at 120 °C under N_2 (g) is unavailable.[59,67,68] By characterizing molecular species formed during the prepolymerization, we determined what constitutes the substrate mixture after the temperature is reduced to 90 °C and N435 is added to reactions at what is considered zero reaction time. Similarly, this provides information for self-catalyzed polymerizations that, after the prepolymerization period, are conducted at 120 °C and 2.5 Torr.

For the 24 h prepolymerization, aliquots were taken from the reaction mixture at 0, 6, 12, 18, and 24 h, after which each sample was analyzed by EMI-MS. The spectra are shown in Figure S1, and the results from these spectra are compiled in Figure 1, where glycerol and sebacate are abbreviated as [G] and [S], respectively. Columns were not used to separate constituent oligomers formed. Instead, all oligomers were eluted at the same time. In other words, all subpeaks of different oligomeric species were eluted at the same time in a combined prominent peak at the retention time of 0.1−0.2 min. This gave specific MS analysis within the same time frame and the results are represented in a single image for comparison.

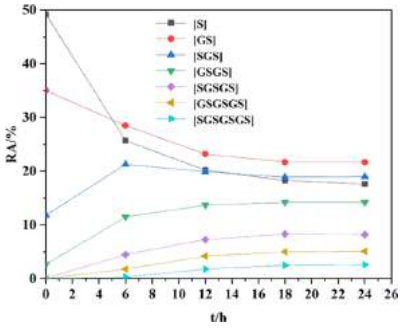

Figure 1. Normalized percent relative abundance (%-RA) of sebacic acid and major oligomers.

Results in Figure 1 use relative abundance (RA) values displayed in MS spectral data, where the *X*- and *Y*-axes are the reaction time and %-RA, respectively. For a selected monomer or oligomeric species with a m/z lower than 1067, its %-RA is normalized, that is, the percent relative abundance is calculated taking the area of the peak corresponding to molecular species and dividing that by the total area of all observed MS peaks corresponding to monomers, dimers, and oligomers. The peaks with m/z higher than 1067 were neglected due to the low peak intensities.

Figure 1 shows that the 0 h sample, which resulted from heating the reaction mixture at 150 °C under N_2 (g) for 1 h, consists primarily of residual sebacic acid (m/z 201.115, 49.2%), dimer [GS] (m/z 275.152, 35.0%), and trimer [SGS] (m/z 459.262, 11.8%). Because the minimum detection limit is m/z 200, glycerol is not detected.

At 6 h, large changes were observed in the relative abundance of most molecular species. The %-RA of sebacic acid and [GS] decreased from 49.2 to 25.7% and 35.0 to 28.5%, respectively. They served as building blocks for increases in [SGS] and [GSGS] (m/z 533.309) from 11.8 to 21.3% and 2.7 to 11.5%. Correspondingly, the relatively larger oligomer [SGSGSGS] (m/z 975.557) increased by only 0.3%.

From 6 to 12 h, differences in the %-RA followed the same trend as 0−6 h, except the magnitude of %-changes decreased significantly. Correspondingly, fluctuations in %-RA further

https://doi.org/10.1021/acs.biomac.1c01351
Biomacromolecules 2022, 23, 398−408

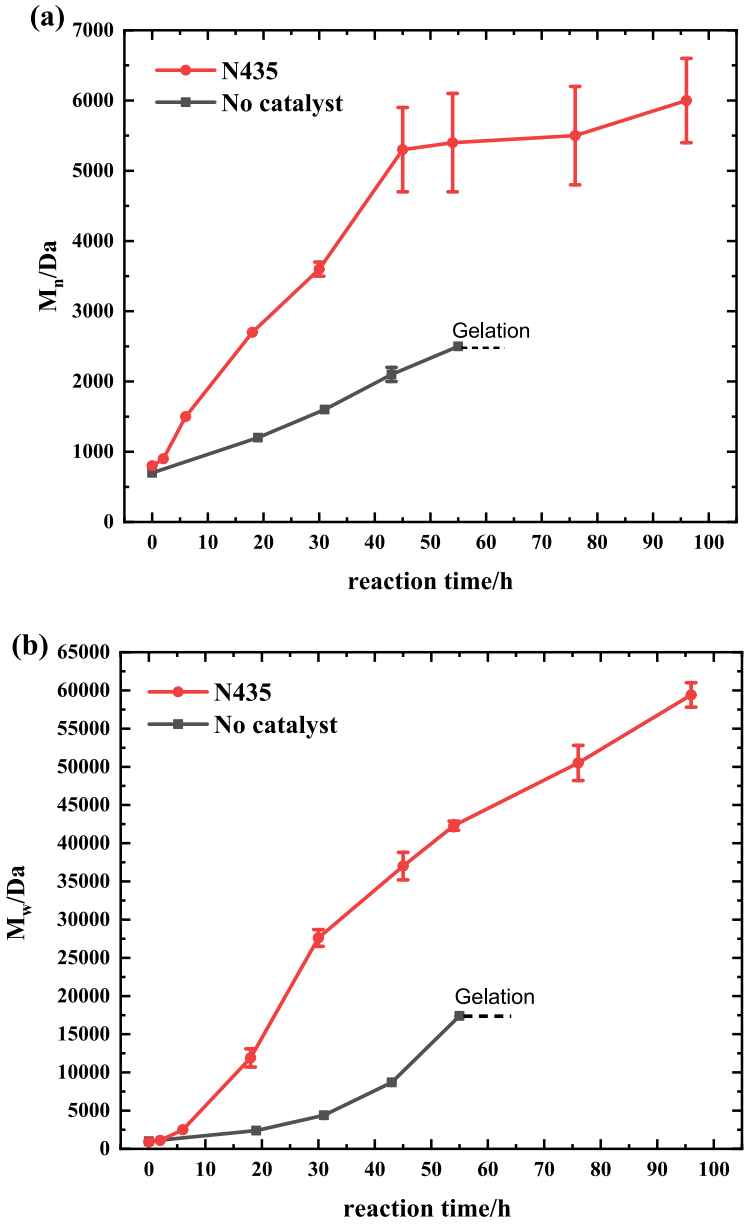

Figure 2. Time-course analysis of (a) M_n of self-catalyzed and N435-catalyzed PGS polymerizations and (b) M_w of self-catalyzed and N435-catalyzed PGS polymerizations. Zero reaction time is taken as after the completion of the initial reaction phases at 150 °C (1 h) followed by 120 °C for 24 h under N_2 (g).

decreased with an increase in the reaction time from 12 to 24 h. Overall, the relative concentrations of molecular species reached plateau values, which is consistent with that, without a vacuum to accelerate water removal and shift the equilibrium, the values attained by 12 h approach those at equilibrium. By 12 h, a large decrease in unreacted sebacic acid occurs with the formation of sebacic acid oligomers that, based on relative abundance values, are predominantly dimers and trimers. Oligomers up to 7 units were observed. Based on these results, the prepolymerization period at 120 h under N_2 (g) can be shortened to 12 h. Furthermore, while at 0 h, the substrate was a solid, but by 12 and 24 h during the prepolymerization, it was transformed to a homogeneous liquid that was a suitable substrate for N435 catalysis.

Time-Course Analysis of Self-Catalyzed and N435-Catalyzed PGS Synthesis. PGS molecular weight was determined for no catalyst and N435-catalyzed polymerizations (Figure 2). Zero reaction time is taken as after the completion of the initial reaction phases at 150 °C (1 h) followed by 120 °C for 24 h under N_2 (g) (prepolymerization conditions). For both polymerizations, M_n and M_w increased with the reaction time. However, at 55 h, the M_n and M_w values of self-catalyzed PGS synthesis reach 2600 and 13 800 g/mol, respectively ($Đ$ = 5.4). For comparison, at the 55 h time point of the enzyme-catalyzed polymerization, M_n and M_w values are

https://doi.org/10.1021/acs.biomac.1c01351
Biomacromolecules 2022, 23, 398−408

5500 and 43 000, respectively. However, gelation of self-catalyzed reactions occurs between 55 and 67 h. For PGS synthesized by N435 catalysis, gel formation did not occur, even at a polymerization time of 96 h. This is attributed to the limited space within the CALB cleft, where the catalytic triad resides. Consequently, internal regions of two chains are not accommodated as they seek to orient within the catalytic site. This phenomenon, in which steric crowding occurs, impedes cross-link reactions.[19] As a result, N435-catalyzed synthesis of PGS continued to 96 h and reached M_n and M_w values of 6000 and 59 400 g/mol, respectively ($Đ$ = 10). The plateau in M_n values with increasing reaction time is a result of increase in viscosity as the functional group conversion increases. This results in a decrease in reactant diffusivity. We expect that by increasing the agitation rate and intensity throughout the reaction mixture using a reactor with overhead mixing and an optimized stirring shaft, it would result in increased M_n and lower $Đ$ values than those reported herein.

Peak Deconvolution Analysis of Higher and Lower Molecular Weight Regions of SEC Traces. PGS synthesized as above have high $Đ$ values and, consequently, SEC traces are typically complex consisting of multiple peaks. To gain further information on the major molecular weight populations present in products, peak deconvolution of SEC traces was conducted. Figure 3 displays the SEC trace of PGS synthesized by N435 catalysis at 96 h. Peaks at 11.8 and 16.8 min correspond to relatively higher and lower molecular weight regions, respectively. SEC deconvolution was performed using OriginPro software (version 2017, OriginLab, Northampton, MA), in which the Gaussian model was applied. OriginPro software also provided the horizontal and vertical axis values of points that formed each fit peak. These values were used with the mathematical equation of the SEC calibration curve, following the Waters company method.[69,70] The green fitting curves display the two deconvoluted peaks corresponding to the higher and lower molecular weight regions of the full chromatograph. The red curve identifies the cumulative peak, which closely resembles the full SEC trace shown in black. Furthermore, the adjusted R^2 was 0.974, indicating that the additive values of deconvoluted peaks provide a good fit for the full SEC trace. Area percentages of the high and low molecular weight deconvoluted traces are 67.6 and 32.4%, respectively. Deconvoluted component traces obtained by the above deconvolution protocol were also determined for the self-catalyzed PGS product at 55 h. The results are listed in Table 1.

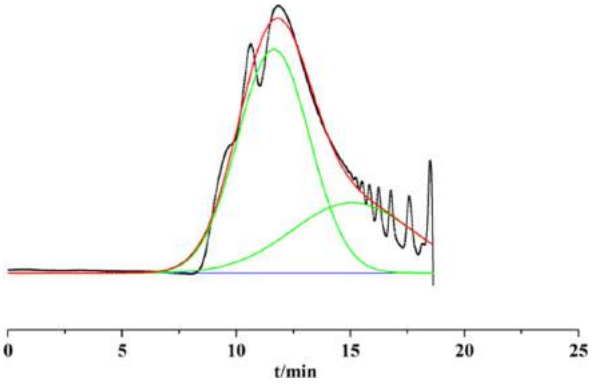

Figure 3. Peak deconvolution of PGS synthesized by N435 catalysis at 96 h. (Black: SEC trace; green: two deconvoluted peaks corresponding to the higher and lower molecular weight regions; red: the cumulative peak.).

Table 1 shows that the M_n of the high molecular weight component peak from N435-catalyzed polymerization (25 200 g/mol) is higher than that obtained by self-catalyzed polymerization (15 200 g/mol). The area ratio of a high molecular weight fraction is higher for the N435-catalyzed polymerization (67.6% vs 23.5%). It follows that the %-area of the lower molecular weight component for the self-catalyzed PGS product at 55 h is more abundant (76.5%) than the corresponding lower molecular weight component for PGS synthesized by N435 catalysis (32.4%). The magnitude of $Đ$ values of components peaks was 1.1−1.7, whereas those of the full SEC traces were 4.2−8.9.

NMR Analysis of PGS. The ^{1}H NMR of PGS synthesized by N435 catalysis at 55 h along with peak assignments is given in Figure 4. Peak assignments were made from those given in previous studies.[46,55,71] The analysis of COSY and HMQC spectra is displayed in Figures 5 and S2, respectively. The full-inverse gated ^{13}C NMR of PGS synthesized with N435 at 55 h and magnifications for peak assignments is shown in Figure S3. DEPT-135 ^{13}C spectrum of PGS synthesized with N435 at 55 h is given in Figures S4−S6 with peak assignments. These peak assignments are based on the previous literature[46,55,71] as well as COSY and HMQC experiments. The full-inverse gated ^{13}C NMR of self-catalyzed PGS at 53 h is shown in Figure S5.

Figure 4 shows assignments of NMR signals that correspond to residual glycerol (Gly), 1-monosubstituted glycerol terminal units (1T), 2-monosubstituted glycerol terminal units (2T), 1,2-disubstituted linear glycerol units (1,2L), 1,3-disubstituted linear glycerol units (1,3L), dendritic units (1,2,3D or D) as well as other protons of sebacic acid repeat units. The assignments of PGS ^{1}H and ^{13}C NMR spectra are consistent with those previously reported.[46,55,71]

The time course of N435-catalyzed PGS synthesis was followed by recording a series of ^{1}H NMR spectra of products formed at reaction times of 0, 19, 31, 43, 55, and 67 h (Figure 6). Expanded regions of the spectra at 3.4−4.5, and 4.8−5.4 ppm are shown in Figure 6. Analysis of the displayed stacked

Table 1. Comparison of Peak Deconvolution Results from PGS Synthesized by Bulk and N435

	full trace			high molecular weight fraction				low molecular weight fraction			
PGS[a]	$M_n \times 10^{-3}$ (g/mol)	$M_w \times 10^{-3}$ (g/mol)	$Đ$	$M_n \times 10^{-3}$ (g/mol)	$M_w \times 10^{-3}$ (g/mol)	$Đ$	area (%)	$M_n \times 10^{-3}$ (g/mol)	$M_w \times 10^{-3}$ (g/mol)	$Đ$	area (%)
96 h N435	6.8	60.8	8.9	25.2	42.8	1.7	67.6	2.3	3.9	1.7	32.4
55 h self-catalyzed	3.1	13.1	4.2	15.2	17.4	1.1	23.5	2.5	3.6	1.4	76.5

[a]Reaction times are after the completion of the prepolymerization step.

https://doi.org/10.1021/acs.biomac.1c01351
Biomacromolecules 2022, 23, 398−408

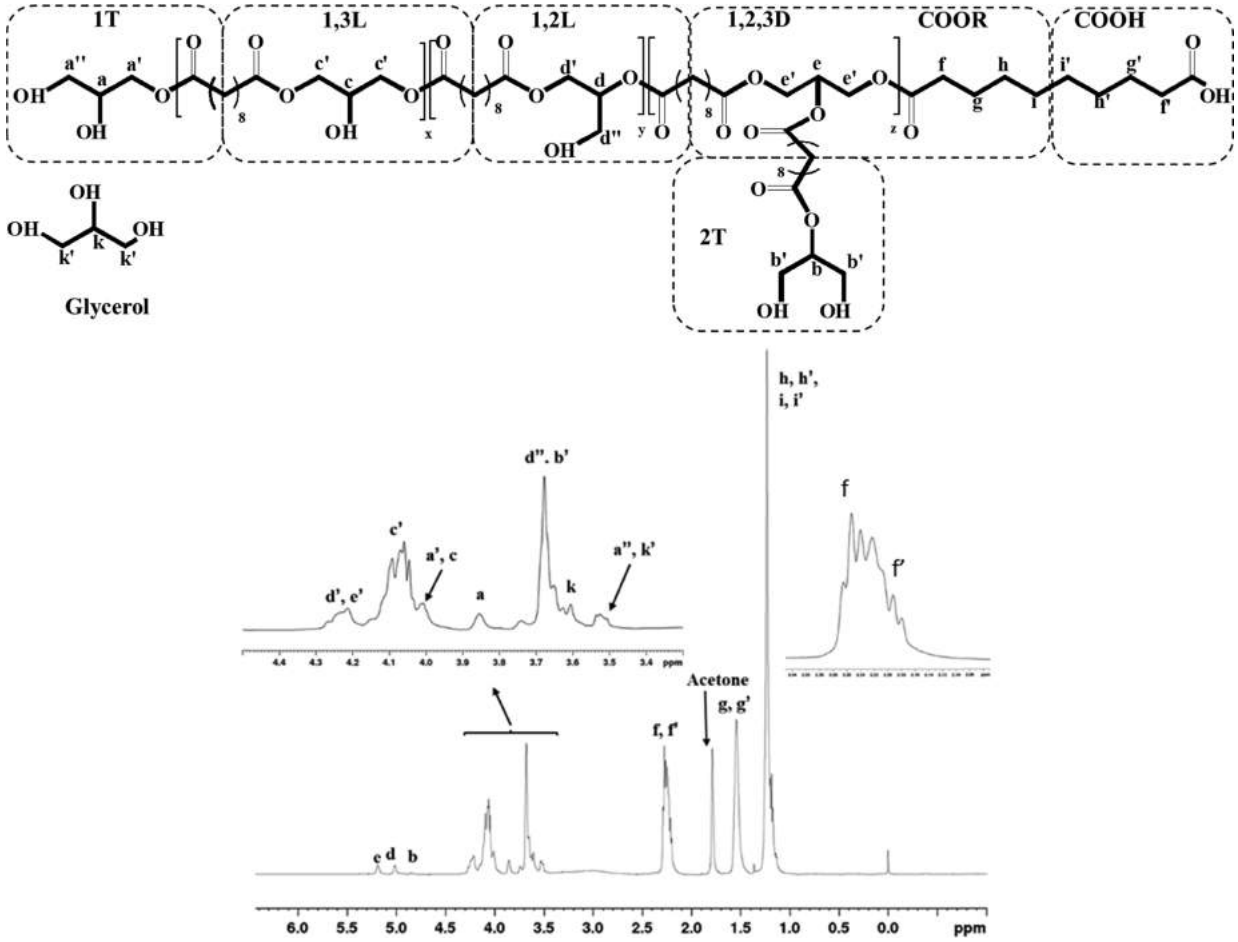

Figure 4. Full ^{1}H NMR of PGS, synthesized by N435 catalysis for 55 h, and an expansion of the region from 3.4 to 4.4 ppm.

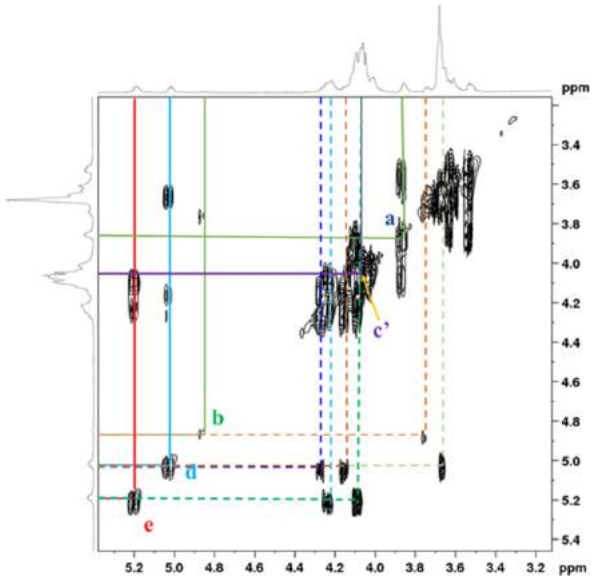

Figure 5. Expanded region (3.3−5.3 ppm) of the COSY spectrum for PGS synthesized via N435 catalysis at 55 h.

NMR plots corresponding to different reaction times allows quantitation spectral changes over times.

The integration intensities corresponding to the proton signals of glycerol units that are nonsubstituted (Gly), 1T, 1,3L, 2T, 1,2L, and 1,2,3D units were used to determine the mol fraction of each for self-catalyzed and N435-catalyzed synthesis of PGS (Tables 2 and 3, respectively). Weak peak intensities for X_{2T}, $X_{1,2L}$, X_{1T}, and X_D result in a deviation between peak intensities for self-catalyzed and enzyme-catalyzed values at time equals zero that are most evident for X_{Gly} and $X_{1,3L}$. However, as the reaction progresses, consistent trends are observed that provide confidence in their significance. Comparisons between PGS synthesized with and without N435 showed that glycerol was more rapidly consumed and reached lower residual glycerol contents for PGS synthesized by N435 catalysis. Also, higher selectivity for substitution at primary hydroxyl units ($X_{1,3L}$) relative to $X_{1,2L}$ disubstitution is evident. Given that the molar ratio of glycerol and sebacate units was 1:1, the tendency to form dendritic units (X_D) was low for PGS synthesized with and without N435 catalysis.

Signals in Figure 4, corresponding to the methylene protons f′, adjacent to the carbonyl of the nonreacted carboxylic acid moieties of sebacic acid, and f, corresponding to esterified sebacic acid groups, are found between 2.2 and 2.4 ppm and

https://doi.org/10.1021/acs.biomac.1c01351
Biomacromolecules 2022, 23, 398−408

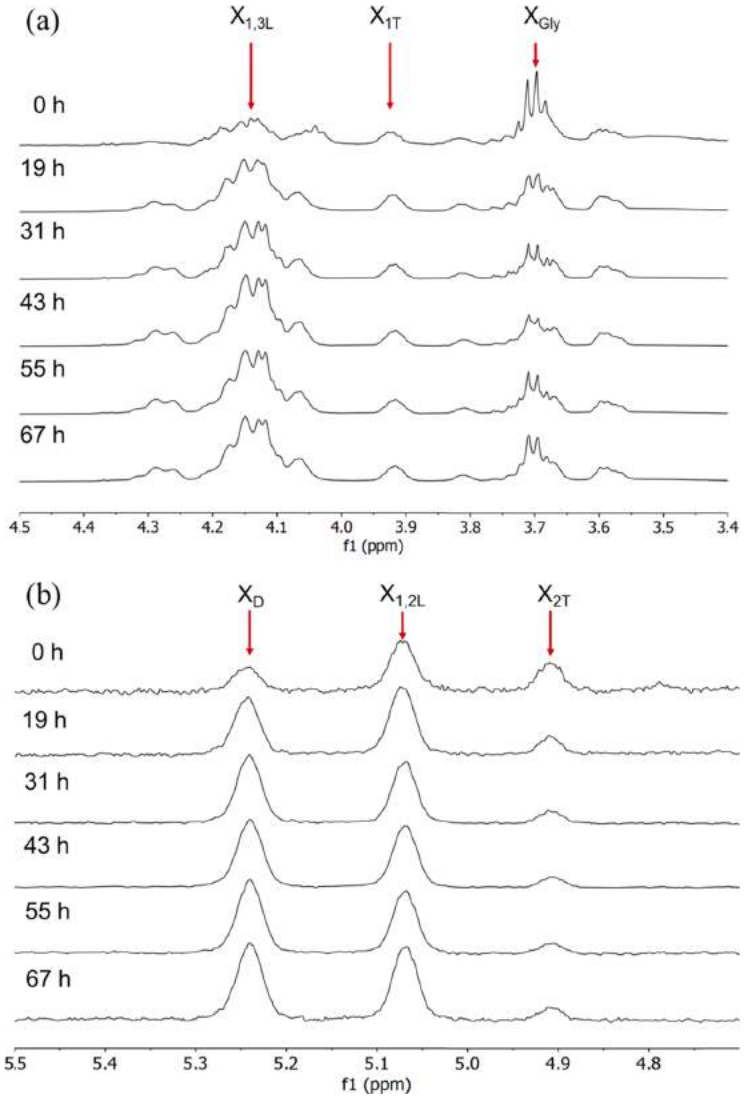

Figure 6. Expansions of the ^{1}H NMR spectra of PGS synthesized by N435 catalysis as a function of time: (a) spectral region from 3.4 to 4.5 ppm reveals the proton signals corresponding to nonreacted glycerol (Gly), 1T and 1,3L units and (b) spectral region from 4.8−5.4 ppm reveals methine protons corresponding to 2T, 1,2L, and 1,2,3D substituted glycerol units.

Table 2. Average Molar Fraction of Glyceridic Species (X_i) in Self-Catalyzed PGS as a Function of the Reaction Time Determined by ^{1}H NMR

reaction time (h)	X_{Gly}	X_{1T}	X_{2T}	$X_{1,3L}$	$X_{1,2L}$	X_D	DS	DB	*p*-OH (%)	*p*-COOH (%)
0	0.30	0.12	0.02	0.51	0.03	0.02	1.83	0.22	42.62	52
2	0.29	0.11	0.02	0.54	0.03	0.02	1.85	0.20	44.03	55
6	0.25	0.10	0.01	0.58	0.04	0.02	1.88	0.18	46.99	59
8	0.21	0.09	0.01	0.65	0.02	0.02	1.89	0.16	49.65	61
30	0.18	0.08	0.01	0.70	0.02	0.02	1.91	0.13	52.61	64
45	0.18	0.08	0.01	0.66	0.04	0.03	1.93	0.15	52.66	67
55	0.17	0.08	0.01	0.67	0.04	0.03	1.93	0.14	53.33	72

that region is expanded. Since f and f′ are not resolved, peak fits are used to estimate their relative intensities. For PGS synthesized by N435 catalysis, the conversion of sebacate carboxylic acid groups to their corresponding ester in PGS chains reached 79% at 55 h, then 82% at 67 h, whereas the self-catalyzed PGS reached 72% at 55 h. At 55 h under enzyme-catalyzed and self-catalyzed reaction conditions, the functional conversion of nonreacted carbonyls is closer in value (79 and 72, respectively). This data demonstrates that N435 catalysis leads to higher sebacic acid functional conversion relative to noncatalyzed PGS at identical reaction time points and, due to the ability to avoid cross-linking, allows extension of the

https://doi.org/10.1021/acs.biomac.1c01351
Biomacromolecules 2022, 23, 398−408

Table 3. Average Molar Fraction of Glyceridic Species (X_i) in PGS Synthesized with N435 as a Function of Reaction Time Determined by ^{1}H NMR

reaction time (h)	X_{Gly}	X_{1T}	X_{2T}	$X_{1,3L}$	$X_{1,2L}$	X_D	DS	DB	*p*-OH (%)	*p*-COOH (%)
0	0.20	0.11	0.01	0.65	0.02	0.01	1.86	0.16	49.67	61
19	0.10	0.10	0.01	0.72	0.04	0.04	1.92	0.17	58.33	71
31	0.09	0.08	0.01	0.75	0.04	0.04	1.95	0.14	59.67	73
43	0.08	0.07	0.01	0.76	0.04	0.04	1.96	0.13	60.00	77
55	0.07	0.07	0.01	0.76	0.04	0.05	1.97	0.14	61.00	79
67	0.06	0.07	0.01	0.77	0.04	0.05	1.97	0.14	61.67	82

reaction time to increase functional conversion. This corresponds to the higher M_n and M_w values of PGS synthesized using N435 (Table 1).

Consistent with the above, calculated conversion of −OH (*p*-OH) groups, using the identical equations in previous literature,[71] is shown in Tables 2 and 3. This calculation assumes that, at a mole ratio of glycerol-to-sebacic acid of 1:1, the upper limit of substitution at glycerol hydroxyl groups is 66.7. At 67 h, for N435-catalyzed PGS synthesis, *p*-OH reached 61.67%, which is 92.5% of the theoretical upper limit (66.7%). In contrast, PGS synthesized without N435 reached 53.33%, which is 80.0% of the theoretical upper limit. These results are consistent with that from sebacic acid carboxyl group conversion.

Fractionating PGS by Precipitation. Precipitation of a polymer allows the attainment of polymer fractions with enhanced contents of higher molecular weight chains. The potential of fractionating PGS by solvent precipitation was explored. For these experiments, methanol, i-propanol, and i-pentanol were selected as nonsolvents. Precipitation was performed by preparing a 50 wt % solution of PGS in THF to which 9-volumes of nonsolvents were slowly added. To increase the recovery of precipitated polymers, turbid solvent/nonsolvent mixtures were maintained for 16 h in the refrigerator. The corresponding %-yields of precipitants are 27.6 ± 6.8, 70.2 ± 8.5, and 40.6 ± 1.2%, respectively (Table 4). Each precipitated fraction from triplicate experiments was analyzed by SEC, and values of M_n, M_w, and $Đ$ were determined. Methanol led to the lowest precipitation yield but gave a precipitant with the highest increases in M_n and M_w. Precipitation with *i*-propanol led to the highest precipitation yield, a moderate increase in M_n, and a 29% decrease in M_w. *i*-Pentanol gave an intermediate precipitation yield, a low increase in M_n (27.1%), and a large decrease in M_w. High increases in M_n (Table 4) reflect that relatively lower molecular weight chains remain in solution during the precipitation. In other words, *i*-propanol and *i*-pentanol may function by decreasing interactions between chains. While the use of methanol as the precipitant resulted in the highest PGS molecular weight with a concurrent decrease in dispersity, the low precipitation yield (27.6%) suggests that further fine-tuning of solvent fractionation conditions is needed.

Table 4. Precipitation Yields and Molecular Weight Averages of the Insoluble Fraction After Solvent Fractionation

N435 PGS	nonsolvent	precipitation yield/%	M_n change (%)	M_w change (%)	$Đ$ change (%)
M_n 6800 (g/mol)	methanol	27.6 ± 6.8	+131.7	+18.3	−47.7
M_w 60 800 (g/mol)	*i*-propanol	70.2 ± 8.5	+60.0	−29.5	−59.6
$Đ$ 8.9	*i*-pentanol	40.6 ± 1.2	+27.1	−47.5	−59.3

CONCLUSIONS

This paper demonstrates that N435 catalysis leads to higher molecular weight PGS than the traditional synthetic route of self-catalyzed condensation polymerization. N435-catalyzed synthesis enabled the preparation of PGS with M_n, M_w, and $Đ$ values of 6000 g/mol, 59 400 g/mol, and 10 at 67 h, respectively. The product formed did not contain a gel fraction. This is attributed to the narrow cleft where the catalytic triad resides, which restricts chain confirmations that would lead to interchain cross-linking reactions. In contrast, PGS synthesized by self-catalysis formed a gel at reaction times between 55 and 67 h since there is little difference in the energetics of reactions leading to cross-linking and linear chain growth. When one of the substrates is solid at the polymerization temperature for an enzyme-catalyzed condensation reaction, a prepolymerization step at an elevated temperature is often carried out to give a homogeneous liquid substrate at the polymerization temperature. However, characterization of the actual substrate for the enzymatic polymerization is rare, if ever carried out. This paper used EMI-MS to determine the evolution of oligomeric species that form during the prepolymerization at 120 °C under N_2 (g) for 24 h. By 12 h, a large decrease in sebacic acid occurs, and oligomers up to 12 units were observed though lower molecular weight species from dimer to tetramer were the most dominant. We determined that the little change in the distribution of oligomeric species occurs beyond 12 h.

Peak deconvolution of PGS synthesized by N435 catalysis gave molecular weight averages and %-contribution of constituent high (67.6%) and low (32.4%) molecular weight product fractions. Integration intensities corresponding to ^{1}H signals of glycerol units were analyzed to provide insights into polymer microstructure changes during the chain growth for N435-catalyzed PGS synthesis. From 0−19 h, X_{Gly} decreased by 2-fold, however, even at 67 h, 6% of glycerol in products remained unreacted. A high preference for primary substitution was observed based on the ratio of $X_{1,3L}/X_{1,2L}$ units as the reaction progressed. The relatively low ratio of X_D units at 67 h (0.05) revealed a relatively low propensity for the formation of dendritic units relative to reactions that further elongate the chain.

The carboxylic acid conversion reached 82% for the N435-catalyzed system which is substantially higher than 72% for the self-catalyzed PGS product. The monomer conversion of −OH (*p*-OH) is also higher for N435 catalysis. This is consistent with the relatively higher molecular weights of PGS synthesized by N435 catalysis.

https://doi.org/10.1021/acs.biomac.1c01351
Biomacromolecules 2022, 23, 398−408

Solvent precipitation was an effective strategy to increase PGS molecular weight while reducing the dispersity value.

■ ASSOCIATED CONTENT

Supporting Information

The Supporting Information is available free of charge at https://pubs.acs.org/doi/10.1021/acs.biomac.1c01351.

Relative percentages of linear, terminal, and dendritic units in the hyperbranched glycerol copolyesters, NMR analysis, and additional tables and figures (PDF)

■ AUTHOR INFORMATION

Corresponding Author

Richard A. Gross − *Department of Chemistry and Chemical Biology and Center for Biotechnology and Interdisciplinary Studies, Rensselaer Polytechnic Institute, Troy, New York 12180, United States; Department of Chemical and Biological Engineering and Center for Biotechnology and Interdisciplinary Studies, Department of Biomedical Engineering and Center for Biotechnology and Interdisciplinary Studies, and Department of Biology and Center for Biotechnology and Interdisciplinary Studies, Rensselaer Polytechnic Institute, Troy, New York 12180, United States;* orcid.org/0000-0002-5050-3162; Email: grossr@rpi.edu; Fax: (518) 276-3734

Authors

Zhuoyuan Ning − *Department of Chemistry and Chemical Biology and Center for Biotechnology and Interdisciplinary Studies, Rensselaer Polytechnic Institute, Troy, New York 12180, United States; School of Chemical Engineering, Zhengzhou University, Zhengzhou 450001 Henan, P. R. China*

Kening Lang − *Department of Chemistry and Chemical Biology and Center for Biotechnology and Interdisciplinary Studies, Rensselaer Polytechnic Institute, Troy, New York 12180, United States*

Ke Xia − *Department of Chemistry and Chemical Biology and Center for Biotechnology and Interdisciplinary Studies, Rensselaer Polytechnic Institute, Troy, New York 12180, United States*

Robert J. Linhardt − *Department of Chemistry and Chemical Biology and Center for Biotechnology and Interdisciplinary Studies, Rensselaer Polytechnic Institute, Troy, New York 12180, United States; Department of Chemical and Biological Engineering and Center for Biotechnology and Interdisciplinary Studies, Department of Biomedical Engineering and Center for Biotechnology and Interdisciplinary Studies, and Department of Biology and Center for Biotechnology and Interdisciplinary Studies, Rensselaer Polytechnic Institute, Troy, New York 12180, United States;* orcid.org/0000-0003-2219-5833

Complete contact information is available at: https://pubs.acs.org/10.1021/acs.biomac.1c01351

Author Contributions

#Z.N. and K.L. contributed equally to this work.

Funding

The authors are profoundly grateful to funding from the Rensselaer Polytechnic Institute Biocatalysis and Bioprocessing Constellation.

Notes

The authors declare no competing financial interest.

■ REFERENCES

(1) Ramakrishna, S.; Mayer, J.; Wintermantel, E.; Leong, K. W. Biomedical Applications of Polymer-Composite Materials: A Review. *Compos. Sci. Technol.* **2001**, *61*, 1189−1224.

(2) Song, R.; Murphy, M.; Li, C.; Ting, K.; Soo, C.; Zheng, Z. Current Development of Biodegradable Polymeric Materials for Biomedical Applications. *Drug Des. Dev. Ther.* **2018**, *12*, 3117−3145.

(3) Lang, K.; Sánchez-Leija, R. J.; Gross, R. A.; Linhardt, R. J. Review on the Impact of Polyols on the Properties of Bio-Based Polyesters. *Polymers* **2020**, *12*, No. 2969.

(4) Kerativitayanan, P.; Tatullo, M.; Khariton, M.; Joshi, P.; Perniconi, B.; Gaharwar, A. K. Nanoengineered Osteoinductive and Elastomeric Scaffolds for Bone Tissue Engineering. *ACS Biomater. Sci. Eng.* **2017**, *3*, 590−600.

(5) Yeh, Y.-C.; Highley, C. B.; Ouyang, L.; Burdick, J. A. 3D Printing of Photocurable Poly(Glycerol Sebacate) Elastomers. *Biofabrication* **2016**, *8*, No. 045004.

(6) Tallawi, M.; Dippold, D.; Rai, R.; D'Atri, D.; Roether, J. A.; Schubert, D. W.; Rosellini, E.; Engel, F. B.; Boccaccini, A. R. Novel PGS/PCL Electrospun Fiber Mats with Patterned Topographical Features for Cardiac Patch Applications. *Mater. Sci. Eng. C* **2016**, *69*, 569−576.

(7) Boutry, C. M.; Nguyen, A.; Lawal, Q. O.; Chortos, A.; Rondeau-Gagné, S.; Bao, Z. Pressure Sensors: A Sensitive and Biodegradable Pressure Sensor Array for Cardiovascular Monitoring. *Adv. Mater.* **2015**, *27*, 6953.

(8) Merle, B.; Kraus, X.; Tallawi, M.; Scharfe, B.; El Fray, M.; Aifantis, K. E.; Boccaccini, A. R.; Göken, M. Dynamic Mechanical Characterization of Poly(Glycerol Sebacate)/Poly(Butylene Succinate-Butylene Dilinoleate) Blends for Cardiac Tissue Engineering by Flat Punch Nanoindentation. *Mater. Lett.* **2018**, *221*, 115−118.

(9) Zhu, C.; Rodda, A. E.; Truong, V. X.; Shi, Y.; Zhou, K.; Haynes, J. M.; Wang, B.; Cook, W. D.; Forsythe, J. S. Increased Cardiomyocyte Alignment and Intracellular Calcium Transients Using Micropatterned and Drug-Releasing Poly(Glycerol Sebacate) Elastomers. *ACS Biomater. Sci. Eng.* **2018**, *4*, 2494−2504.

(10) Hu, J.; Kai, D.; Ye, H.; Tian, L.; Ding, X.; Ramakrishna, S.; Loh, X. J. Electrospinning of Poly(Glycerol Sebacate)-Based Nanofibers for Nerve Tissue Engineering. *Mater. Sci. Eng. C* **2017**, *70*, 1089−1094.

(11) Jiang, L.; Jiang, Y.; Stiadle, J.; Wang, X.; Wang, L.; Li, Q.; Shen, C.; Thibeault, S. L.; Turng, L.-S. Electrospun Nanofibrous Thermoplastic Polyurethane/Poly(Glycerol Sebacate) Hybrid Scaffolds for Vocal Fold Tissue Engineering Applications. *Mater. Sci. Eng. C* **2019**, *94*, 740−749.

(12) Hsu, C.-N.; Lee, P.-Y.; Tuan-Mu, H.-Y.; Li, C.-Y.; Hu, J.-J. Fabrication of a Mechanically Anisotropic Poly(Glycerol Sebacate) Membrane for Tissue Engineering: Fabrication of an Anisotropic PGS Membrane. *J. Biomed. Mater. Res. B* **2018**, *106*, 760−770.

(13) Frydrych, M.; Román, S.; MacNeil, S.; Chen, B. Biomimetic Poly(Glycerol Sebacate)/Poly(l-Lactic Acid) Blend Scaffolds for Adipose Tissue Engineering. *Acta Biomater.* **2015**, *18*, 40−49.

(14) Mitsak, A. G.; Dunn, A. M.; Hollister, S. J. Mechanical Characterization and Non-Linear Elastic Modeling of Poly(Glycerol Sebacate) for Soft Tissue Engineering. *J. Mech. Behav. Biomed. Mater.* **2012**, *11*, 3−15.

(15) Wang, Y.; Ameer, G. A.; Sheppard, B. J.; Langer, R. A Tough Biodegradable Elastomer. *Nat. Biotechnol.* **2002**, *20*, 602−606.

(16) Huang, P.; Bi, X.; Gao, J.; Sun, L.; Wang, S.; Chen, S.; Fan, X.; You, Z.; Wang, Y. Phosphorylated Poly(Sebacoyl Diglyceride) - a Phosphate Functionalized Biodegradable Polymer for Bone Tissue Engineering. *J. Mater. Chem. B* **2016**, *4*, 2090−2101.

(17) Yoon, S.; Chen, B. Elastomeric and PH-Responsive Hydrogels Based on Direct Crosslinking of the Poly(Glycerol Sebacate) Pre-Polymer and Gelatin. *Polym. Chem.* **2018**, *9*, 3727−3740.

(18) Ning, Z. Y.; Zhang, Q. S.; Wu, Q. P.; Li, Y. Z.; Ma, D. X.; Chen, J. Z. Efficient Synthesis of Hydroxyl Functioned Polyesters from

Natural Polyols and Sebacic Acid. *Chin. Chem. Lett.* **2011**, *22*, 635−638.
(19) Yang, Y.; Lu, W.; Cai, J.; Hou, Y.; Ouyang, S.; Xie, W.; Gross, R. A. Poly(Oleic Diacid-Co-Glycerol): Comparison of Polymer Structure Resulting from Chemical and Lipase Catalysis. *Macromolecules* **2011**, *44*, 1977−1985.
(20) Zhang, Y.-R.; Spinella, S.; Xie, W.; Cai, J.; Yang, Y.; Wang, Y.-Z.; Gross, R. A. Polymeric Triglyceride Analogs Prepared by Enzyme-Catalyzed Condensation Polymerization. *Eur. Polym. J.* **2013**, *49*, 793−803.
(21) Taresco, V.; Creasey, R. G.; Kennon, J.; Mantovani, G.; Alexander, C.; Burley, J. C.; Garnett, M. C. Variation in Structure and Properties of Poly(Glycerol Adipate) via Control of Chain Branching during Enzymatic Synthesis. *Polymer* **2016**, *89*, 41−49.
(22) Kulshrestha, A. S.; Gao, W.; Gross, R. A. Glycerol Copolyesters: Control of Branching and Molecular Weight Using a Lipase Catalyst. *Macromolecules* **2005**, *38*, 3193−3204.
(23) Fu, H.; Kulshrestha, A. S.; Gao, W.; Gross, R. A.; Baiardo, M.; Scandola, M. Physical Characterization of Sorbitol or Glycerol Containing Aliphatic Copolyesters Synthesized by Lipase-Catalyzed Polymerization. *Macromolecules* **2003**, *36*, 9804−9808.
(24) Kumar, A.; Kulshrestha, A. S.; Gao, W.; Gross, R. A. Versatile Route to Polyol Polyesters by Lipase Catalysis. *Macromolecules* **2003**, *36*, 8219−8221.
(25) Mahapatro, A.; Kalra, B.; Kumar, A.; Gross, R. A. Lipase-Catalyzed Polycondensations: Effect of Substrates and Solvent on Chain Formation, Dispersity, and End-Group Structure. *Biomacromolecules* **2003**, *4*, 544−551.
(26) Bilal, M. H.; Prehm, M.; Njau, A. E.; Samiullah, M. H.; Meister, A.; Kressler, J. Enzymatic Synthesis and Characterization of Hydrophilic Sugar Based Polyesters and Their Modification with Stearic Acid. *Polymers* **2016**, *8*, No. 80.
(27) Gustini, L.; Noordover, B. A. J.; Gehrels, C.; Dietz, C.; Koning, C. E. Enzymatic Synthesis and Preliminary Evaluation as Coating of Sorbitol-Based, Hydroxy-Functional Polyesters with Controlled Molecular Weights. *Eur. Polym. J.* **2015**, *67*, 459−475.
(28) Hu, J.; Gao, W.; Kulshrestha, A.; Gross, R. A. "Sweet Polyesters": Lipase-Catalyzed Condensation− Polymerizations of Alditols. *Macromolecules* **2006**, *39*, 6789−6792.
(29) Liang, L.; Long, J.; Li, G. Lipase-Catalyzed Synthesis of Hyperbranched Polyester Improved by Autocatalytic Prepolymerization Process. *J. Appl. Polym. Sci.* **2019**, *136*, No. 47221.
(30) Mahapatro, A.; Kumar, A.; Kalra, B.; Gross, R. A. Solvent-Free Adipic Acid/1,8-Octanediol Condensation Polymerizations Catalyzed by Candida antartica Lipase B. *Macromolecules* **2004**, *37*, 35−40.
(31) Rao, Z. K.; Ni, H. L.; Li, Y.; Zhu, H. Y.; Liu, Y.; Hao, J. Y. Macroscopic Scaffold Control for Lipase-Catalyzed Dendritic Polyol-Polyesters. *Macromol. Chem. Phys.* **2019**, *220*, No. 1900048.
(32) Natarajan, J.; Madras, G.; Chatterjee, K. Localized Delivery and Enhanced Osteogenic Differentiation with Biodegradable Galactitol Polyester Elastomers. *RSC Adv.* **2016**, *6*, 61492−61504.
(33) Xu, F.; Zhong, J.; Qian, X.; Li, Y.; Lin, X.; Wu, Q. Multifunctional Poly(Amine-Ester)-Type Hyperbranched Polymers: Lipase-Catalyzed Green Synthesis, Characterization, Biocompatibility, Drug Loading and Anticancer Activity. *Polym. Chem.* **2013**, *4*, 3480.
(34) Zhu, C.; Rodda, A. E.; Truong, V. X.; Shi, Y.; Zhou, K.; Haynes, J. M.; Wang, B.; Cook, W. D.; Forsythe, J. S. Increased Cardiomyocyte Alignment and Intracellular Calcium Transients Using Micropatterned and Drug-Releasing Poly(Glycerol Sebacate) Elastomers. *ACS Biomater. Sci. Eng.* **2018**, *4*, 2494−2504.
(35) Loh, X. J.; Abdul Karim, A.; Owh, C. Poly(Glycerol Sebacate) Biomaterial: Synthesis and Biomedical Applications. *J. Mater. Chem. B* **2015**, *3*, 7641−7652.
(36) Rai, R.; Tallawi, M.; Grigore, A.; Boccaccini, A. R. Synthesis, Properties and Biomedical Applications of Poly(Glycerol Sebacate) (PGS): A Review. *Prog. Polym. Sci.* **2012**, *37*, 1051−1078.
(37) Capristo, E.; Mingrone, G.; De Gaetano, A.; Addolorato, G.; Greco, A. V.; Gasbarrini, G. A New HPLC Method for the Direct Analysis of Triglycerides of Dicarboxylic Acids in Biological Samples. *Clin. Chim. Acta* **1999**, *289*, 11−21.
(38) Xue, L.-L.; Chen, H.-H.; Jiang, J.-G. Implications of glycerol metabolism for lipid production. *Prog. Lipid Res.* **2017**, *68*, 12−25.
(39) Shan, A. H.; Jiang, L.; Li, Z. Biodegradable Polyester Thermogelling System as Emerging Materials for Therapeutic Applications. *Macromol. Mater. Eng.* **2018**, *303*, No. 1700656.
(40) Chen, Q.; Yang, X.; Li, Y. A Comparative Study on in Vitro Enzymatic Degradation of Poly(Glycerol Sebacate) and Poly(Xylitol Sebacate). *RSC Adv.* **2012**, *2*, 4125.
(41) Gross, R. A.; Kumar, A.; Kalra, B. Polymer Synthesis by In Vitro Enzyme Catalysis. *Chem. Rev.* **2001**, *101*, 2097−2124.
(42) You, Z.; Bi, X.; Wang, Y. Fine Control of Polyester Properties via Epoxide ROP Using Monomers Carrying Diverse Functional Groups. *Macromol. Biosci.* **2012**, *12*, 822−829.
(43) You, Z.; Bi, X.; Jeffries, E. M.; Wang, Y. A Biocompatible, Metal-Free Catalyst and Its Application in Microwave-Assisted Synthesis of Functional Polyesters. *Polym. Chem.* **2012**, *3*, 384−389.
(44) Hu, J.; Gao, W.; Kulshrestha, A.; Gross, R. A. "Sweet Polyesters": Lipase-Catalyzed Condensation−Polymerizations of Alditols. *Macromolecules* **2006**, *39*, 6789−6792.
(45) Rai, R.; Tallawi, M.; Barbani, N.; Frati, C.; Madeddu, D.; Cavalli, S.; Graiani, G.; Quaini, F.; Roether, J. A.; Schubert, D. W.; Rosellini, E.; Boccaccini, A. R. Biomimetic Poly(Glycerol Sebacate) (PGS) Membranes for Cardiac Patch Application. *Mater. Sci. Eng. C* **2013**, *33*, 3677−3687.
(46) Li, Y.; Cook, W. D.; Moorhoff, C.; Huang, W. C.; Chen, Q. Z. Synthesis, Characterization and Properties of Biocompatible Poly (Glycerol Sebacate) Pre-polymer and Gel. *Polym. Int.* **2013**, *62*, 534−547.
(47) Ye, H.; Owh, C.; Loh, X. J. A Thixotropic Polyglycerol Sebacate-Based Supramolecular Hydrogel Showing UCST Behavior. *RSC Adv.* **2015**, *5*, 48720−48728.
(48) Yan, Y.; Potts, M.; Jiang, Z.; Sencadas, V. Synthesis of Highly-Stretchable Graphene − Poly(Glycerol Sebacate) Elastomeric Nanocomposites Piezoresistive Sensors for Human Motion Detection Applications. *Compos. Sci. Technol.* **2018**, *162*, 14−22.
(49) Sundback, C. A.; McFadden, J.; Hart, A.; Kulig, K. M.; Wieland, A. M.; Pereira, M. J. N.; Pomerantseva, I.; Hartnick, C. J.; Masiakos, P. T. Behavior of Poly(Glycerol Sebacate) Plugs in Chronic Tympanic Membrane Perforations. *J. Biomed. Mater. Res. B* **2012**, *100*, 1943−1954.
(50) Conejero-García, Á.; Gimeno, H. R.; Sáez, Y. M.; Vilariño-Feltrer, G.; Ortuño-Lizarán, I.; Vallés-Lluch, A. Correlating Synthesis Parameters with Physicochemical Properties of Poly(Glycerol Sebacate). *Eur. Polym. J.* **2017**, *87*, 406−419.
(51) Li, X.; Hong, A. T.-L.; Naskar, N.; Chung, H.-J. Criteria for Quick and Consistent Synthesis of Poly(Glycerol Sebacate) for Tailored Mechanical Properties. *Biomacromolecules* **2015**, *16*, 1525−1533.
(52) Yeh, Y.-C.; Ouyang, L.; Highley, C. B.; Burdick, J. A. Norbornene-modified poly (glycerol sebacate) as a photocurable and biodegradable elastomer. *Polym. Chem.* **2017**, *8*, 5091−5099.
(53) Ninh, C.; Bettinger, C. J. Reconfigurable Biodegradable Shape-Memory Elastomers via Diels-Alder Coupling. *Biomacromolecules* **2013**, *14*, 2162−2170.
(54) Chai, Y.; Lin, D.; Ma, Y.; Yuan, Y.; Liu, C. RhBMP-2 Loaded MBG/PEGylated Poly(Glycerol Sebacate) Composite Scaffolds for Rapid Bone Regeneration. *J. Mater. Chem. B* **2017**, *5*, 4633−4647.
(55) Moorhoff, C.; Li, Y.; Cook, W. D.; Braybrook, C.; Chen, Q.-Z. Characterization of the Prepolymer and Gel of Biocompatible Poly(Xylitol Sebacate) in Comparison with Poly(Glycerol Sebacate) Using a Combination of Mass Spectrometry and Nuclear Magnetic Resonance: NMR and MS Characterization of PGS and PXS. *Polym. Int.* **2015**, *64*, 668−688.
(56) Sander, M. M.; Ferreira, C. A. Synthesis and Characterization of a Conductive and Self-Healing Composite. *Synth. Met.* **2018**, *243*, 58−66.

https://doi.org/10.1021/acs.biomac.1c01351
Biomacromolecules 2022, 23, 398−408

(57) Tallawi, M.; Rai, R.; R-Gleixner, M.; Roerick, O.; Weyand, M.; Roether, J. A.; Schubert, D. W.; Kozlowska, A.; Fray, M. E.; Merle, B.; Göken, M.; Aifantis, K.; Boccaccini, A. R. Poly(Glycerol Sebacate)\poly(Butylene Succinate-Dilinoleate) Blends as Candidate Materials for Cardiac Tissue Engineering. *Macromol. Symp.* **2013**, *334*, 57−67.
(58) Tevlek, A.; Hosseinian, P.; Ogutcu, C.; Turk, M.; Aydin, H. M. Bi-Layered Constructs of Poly(Glycerol-Sebacate)-β-Tricalcium Phosphate for Bone-Soft Tissue Interface Applications. *Mater. Sci. Eng. C* **2017**, *72*, 316−324.
(59) Gross, R. A.; Ganesh, M.; Lu, W. Enzyme-Catalysis Breathes New Life into Polyester Condensation Polymerizations. *Trends Biotechnol.* **2010**, *28*, 435−443.
(60) Yu, Y.; Wu, D.; Liu, C.; Zhao, Z.; Yang, Y.; Li, Q. Lipase/Esterase-Catalyzed Synthesis of Aliphatic Polyesters via Polycondensation: A Review. *Process Biochem.* **2012**, *47*, 1027−1036.
(61) Sahoo, B.; Bhattacharya, A.; Fu, H.; Gao, W.; Gross, R. A. Influence of PEG Endgroup and Molecular Weight on Its Reactivity for Lipase-Catalyzed Polyester Synthesis. *Biomacromolecules* **2006**, *7*, 1042−1048.
(62) Yoon, K. R.; Hong, S.-P.; Kong, B.; Choi, I. S. Polycondensation of Sebacic Acid with Primary and Secondary Hydroxyl Groups Containing Diols Catalyzed by Candida Antarctica Lipase B. *Synth. Commun.* **2012**, *42*, 3504−3512.
(63) Lang, K.; Bhattacharya, S.; Ning, Z.; Sánchez-Leija, R. J.; Bramson, M. T. K.; Centore, R.; Corr, D. T.; Linhardt, R. J.; Gross, R. A. Enzymatic Polymerization of Poly(Glycerol-1,8-Octanediol-Sebacate): Versatile Poly(Glycerol Sebacate) Analogues That Form Monocomponent Biodegradable Fiber Scaffolds. *Biomacromolecules* **2020**, *21*, 3197−3206.
(64) Roy, D.; Giller, C. B.; Hogan, T. E.; Roland, C. M. The Rheology and Gelation of Bidisperse 1,4-Polybutadiene. *Polymer* **2015**, *81*, 111−118.
(65) PubChem. Sebacic Acid. https://pubchem.ncbi.nlm.nih.gov/compound/Sebacic-acid (accessed June 01, 2021).
(66) Azim, H.; Dekhterman, A.; Jiang, Z.; Gross, R. A. Candida Antarctica Lipase B-Catalyzed Synthesis of Poly(Butylene Succinate): Shorter Chain Building Blocks Also Work. *Biomacromolecules* **2006**, *7*, 3093−3097.
(67) Gkountela, C.; Rigopoulou, M.; Barampouti, E. M.; Vouyiouka, S. Enzymatic Prepolymerization Combined with Bulk Post-Polymerization towards the Production of Bio-Based Polyesters: The Case of Poly(Butylene Succinate). *Eur. Polym. J.* **2021**, *143*, No. 110197.
(68) Vouyiouka, S. N.; Topakas, E.; Katsini, A.; Papaspyrides, C. D.; Christakopoulos, P. A Green Route for the Preparation of Aliphatic Polyesters via Lipase-Catalyzed Prepolymerization and Low-Temperature Postpolymerization: A Green Route for the Preparation of Aliphatic Polyesters via Lipase-Catalyzed. *Macromol. Mater. Eng.* **2013**, *298*, 679−689.
(69) Azim, H.; Dekhterman, A.; Jiang, Z.; Gross, R. A. CandidaantarcticaLipase B-Catalyzed Synthesis of Poly(Butylene Succinate): Shorter Chain Building Blocks Also Work. *Biomacromolecules* **2006**, *7*, 3093−3097.
(70) Lesec, J.; Millequant, M.; Patin, M.; Teyssie, P. Star-Branched Polymers in Multidetection Gel Permeation Chromatography. In *Advances in Chemistry*; American Chemical Society, 1995; pp 167−179.
(71) Perin, G. B.; Felisberti, M. I. Enzymatic Synthesis of Poly(Glycerol Sebacate): Kinetics, Chain Growth, and Branching Behavior. *Macromolecules* **2020**, *53*, 7925−7935.

https://doi.org/10.1021/acs.biomac.1c01351
Biomacromolecules 2022, 23, 398−408